

# Application of the Redox-Transmetalation Procedure to Access Divalent Lanthanide and Alkaline-Earth NHC Complexes\*\*

Noah Schwarz,<sup>[a]</sup> Xiaofei Sun,<sup>[a]</sup> Ravi Yadav,<sup>[a]</sup> Ralf Köppe,<sup>[a]</sup> Thomas Simler,<sup>\*,[a, b]</sup> and Peter W. Roesky<sup>\*,[a]</sup>

**Abstract:** Divalent lanthanide and alkaline-earth complexes supported by N-heterocyclic carbene (NHC) ligands have been accessed by redox-transmetalation between air-stable NHC-Ag<sup>I</sup> complexes and the corresponding metals. By using the small ligand 1,3-dimethylimidazol-2-ylidene (IMe), two series of isostructural complexes were obtained: the tetra-NHC complexes [LnI<sub>2</sub>(IMe)<sub>4</sub>] (Ln=Eu and Sm) and the bis-NHC complexes [MI<sub>2</sub>(IMe)<sub>2</sub>(THF)<sub>2</sub>] (M=Yb, Ca and Sr). In the former, distortions in the NHC coordination were found to originate from intermolecular repulsions in the solid state. Application of the redox-transmetalation strategy with the bulkier 1,3-

dimesitylimidazol-2-ylidene (IMes) ligand yielded [SrI<sub>2</sub>(IMes)(THF)<sub>3</sub>], while using a similar procedure with Ca metal led to [CaI<sub>2</sub>(THF)<sub>4</sub>] and uncoordinated IMes. DFT calculations were performed to rationalise the selective formation of the bis-NHC adduct in [SrI<sub>2</sub>(IMe)<sub>2</sub>(THF)<sub>2</sub>] and the tetra-NHC adduct in [SmI<sub>2</sub>(IMe)<sub>4</sub>]. Since the results in the gas phase point towards preferential formation of the tetra-NHC complexes for both metal centres, the differences between both arrangements are a result of solid-state effects such as slightly different packing forces.

## Introduction

Since the discovery of isolable free N-heterocyclic carbenes (NHCs) by Arduengo and co-workers in 1991,<sup>[1]</sup> the versatility of these ligands has been evidenced by their ability to coordinate to almost all elements of the periodic table. Although early studies mainly focused on NHC complexes of transition metals (TMs) in various oxidation states,<sup>[2]</sup> NHCs have also been successfully used to stabilise main-group compounds<sup>[2b,3]</sup> and coordinate to f-block elements.<sup>[4]</sup> They have been incorporated in functional or adaptable architectures,<sup>[5]</sup> and the corresponding complexes have found applications in catalysis,<sup>[6]</sup> medicinal and materials chemistry.<sup>[7]</sup> Several routes have been established

to access metal-NHC complexes, the most general one corresponding to the metalation of free carbenes, the latter either isolated or generated in situ by deprotonation of the corresponding imidazolium salts (Scheme 1, route a).<sup>[1b,8]</sup> However, free NHCs are generally sensitive towards air and moisture and, in some cases, thermally unstable or decompose over time, which restricts the scope of this methodology.<sup>[9]</sup> Alternatively, the reaction of an imidazolium salt with a metal precursor that possesses a coordinated base is also a common way to synthesise TM-NHC complexes (Scheme 1, route b). In this context, a variety of metal precursors with built-in basic ligands has been used, such as [Pd(OAc)<sub>2</sub>],<sup>[10]</sup> [M(μ-OMe)(cod)]<sub>2</sub> (M=Rh, Ir; cod = 1,5-cyclooctadiene),<sup>[11]</sup> [M{N(SiMe<sub>3</sub>)<sub>2</sub>}<sub>2</sub>] (M=Fe, Co)<sup>[12]</sup> and [Cu(Mes)<sub>5</sub>].<sup>[13]</sup> This route is especially useful when the free carbene is not stable under typical reaction conditions,<sup>[12c]</sup> but it requires an appropriate metal precursor which preparation may be tedious, as is the case for the highly air-sensitive complexes [M{N(SiMe<sub>3</sub>)<sub>2</sub>}<sub>2</sub>] (M=Fe, Co).<sup>[14]</sup>

An alternative and well-established procedure to synthesise TM-NHC complexes is by transmetalation from NHC-Ag<sup>I</sup> complexes (Scheme 1, route c).<sup>[15]</sup> The latter are accessible by the straightforward reaction of Ag<sub>2</sub>O with the corresponding imidazolium salts and have the advantage to be usually air stable, which simplifies their purification. This transmetalation procedure is especially adapted for NHC transfer to late TMs but does not proceed well with electropositive metal centres including early TMs, main-group metals and lanthanides.<sup>[4a,16]</sup> Although carbene transfer reactions from NHC-Ag<sup>I</sup> complexes to TMs typically proceed without any change in the oxidation states of the involved metals, in rare cases, oxidation of the TM precursor has been observed while the Ag<sup>I</sup> centre was reduced

[a] N. Schwarz, X. Sun, Dr. R. Yadav, Dr. R. Köppe, Dr. T. Simler, Prof. Dr. P. W. Roesky  
Institute of Inorganic Chemistry  
Karlsruhe Institute of Technology (KIT)  
Engesserstraße 15, 76131, Karlsruhe (Germany)  
E-mail: thomas.simler@polytechnique.edu  
roesky@kit.edu

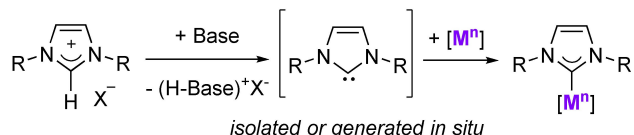
[b] Dr. T. Simler  
Laboratoire de Chimie Moléculaire (LCM)  
CNRS, École Polytechnique  
Institut Polytechnique de Paris, 91120 Palaiseau (France)

[\*\*] NHC=N-heterocyclic carbene.

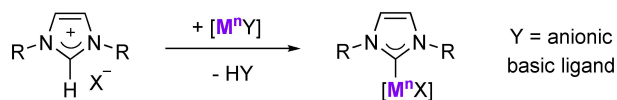
Supporting information for this article is available on the WWW under <https://doi.org/10.1002/chem.202101923>

© 2021 The Authors. Chemistry - A European Journal published by Wiley-VCH GmbH. This is an open access article under the terms of the Creative Commons Attribution Non-Commercial License, which permits use, distribution and reproduction in any medium, provided the original work is properly cited and is not used for commercial purposes.

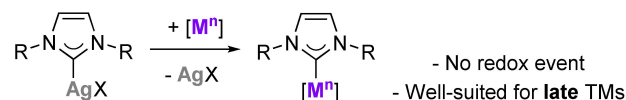
## a) Metalation of free carbene



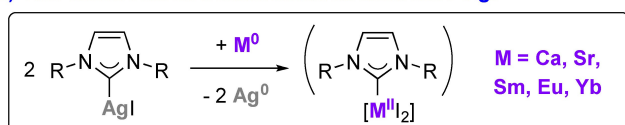
## b) Use of metal precursor with coordinated basic ligand



## c) Standard transmetalation from NHC-AgX



## d) This work: Redox-transmetalation from NHC-AgI



**Scheme 1.** Simplified representation of the routes to access NHC-metal complexes: metalation of free carbene (route a), reaction of an imidazolium salt with a metal precursor featuring a coordinated base (route b), standard transmetalation from an NHC-Ag<sup>I</sup> complex (route c) and redox-transmetalation between an NHC-Ag<sup>I</sup> complex and a zero-valent metal (route d).

to elemental silver. For example, in 2004, Arnold and co-workers reported the synthesis of a Ru<sup>III</sup>-NHC complex upon reaction of the corresponding NHC-Ag<sup>I</sup> complex with a Ru<sup>II</sup> precursor.<sup>[17]</sup> One year later, the synthesis of Rh<sup>III</sup> and Ir<sup>III</sup> complexes upon transmetalation of NHC-silver complexes with the monovalent metal precursors [MCl(coe)<sub>2</sub>]<sub>2</sub> (M=Rh, Ir; coe=cyclooctene) was reported by Peris and co-workers.<sup>[18]</sup> Two other examples of reactions between NHC-Ag<sup>I</sup> complexes and metal precursors that resulted in the oxidation of the latter with formation of elemental silver were reported, leading to the formation of oxidised Cr<sup>III</sup> and Au<sup>III</sup> NHC complexes.<sup>[19]</sup> In all these examples, the observed redox-transmetalation reactivity was unexpected and found to highly depend on the nature of the ligands. To the best of our knowledge, in only one previous report, this unusual reactivity of NHC-Ag<sup>I</sup> compounds has been suggested as a possible way to synthesise late TMs (Fe–Cu) complexes supported by functionalised bis-NHC ligands.<sup>[20]</sup> In addition, the successful redox-transmetalation between an NHC-Hg<sup>II</sup> complex and a Pd<sup>0</sup> species has been reported by Baker et al., leading to the corresponding NHC-Pd<sup>II</sup> complex.<sup>[21]</sup> However, further examples of rational application of the redox-transmetalation procedure with NHC ligands (Scheme 1, route d) are still missing, especially examples involving electropositive metal centres. It should be noted that redox-transmetalation (and possible further protolysis) processes have been a common way to synthesise lanthanide complexes with a variety of ligands,<sup>[22]</sup> such as cyclopentadienyls,<sup>[23]</sup> amides,<sup>[24]</sup> aryloxides,<sup>[25]</sup> pyrazolates<sup>[26]</sup> and thiolates.<sup>[27]</sup> While most studies, pioneered by

Deacon, Junk and co-workers, have focused on organometallic thallium(I),<sup>[23a,b]</sup> mercury(II)<sup>[28]</sup> and tin transfer reagents,<sup>[24a,29]</sup> a very recent interest has been directed to the use of less toxic bismuth and silver organometallics as partners in redox-transmetalation/protolysis reactions with lanthanide metals.<sup>[30]</sup>

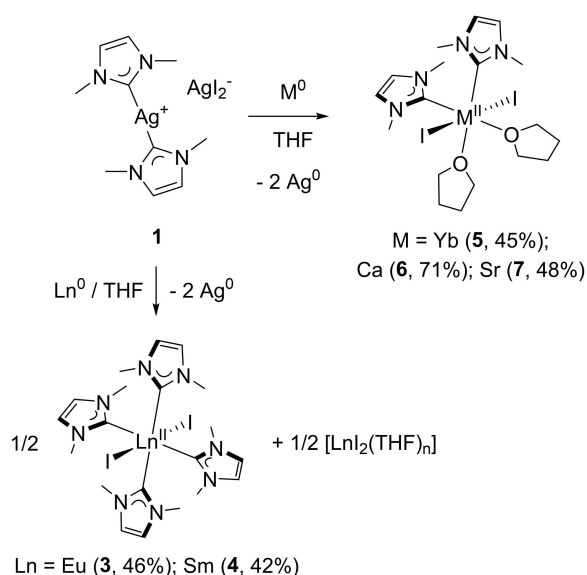
In this context, in a previous communication, we reported the viability of the redox-transmetalation procedure for the synthesis of Ln<sup>II</sup>-IMes (Ln=Eu, Yb; IMes=1,3-dimesitylimidazol-2-ylidene) complexes directly from the corresponding lanthanide metals and NHC-silver complexes.<sup>[31]</sup> Herein, we investigate the generality of this procedure using two different NHC ligands and its applicability to access divalent lanthanide (Sm, Eu, Yb) and alkaline-earth (Ca, Sr) NHC complexes, which cannot typically be obtained using standard (non-redox) transmetalation procedures from NHC-Ag<sup>I</sup> complexes. Through different series of isostructural complexes, a detailed analysis of the coordination behaviour of the NHC ligands has been performed and DFT calculations were carried out to evaluate the differences in the bonding of the IMe ligand between Sm<sup>II</sup> and Sr<sup>II</sup> metal centres.

## Results and Discussion

### Synthesis of divalent lanthanide IMe complexes

To investigate whether the redox-transmetalation procedure could be generalised to other monodentate NHC ligands and electropositive metal centres, the small 1,3-dimethylimidazol-2-ylidene (IMe) ligand was selected for the synthesis of divalent lanthanide and alkaline-earth NHC complexes. Using solid and air-stable NHC silver(I) complexes as a carbene source is especially attractive in the specific case of the IMe ligand, taking into consideration that free IMe is an oily liquid at room temperature that, in addition, slowly decomposes when stored in a neat form.<sup>[9]</sup> In the redox-transmetalation methodology, reductive cleavage of the M–C<sup>NHC</sup> bond occurs,<sup>[32]</sup> resulting into the in situ generation and metalation of a free NHC ligand.<sup>[31]</sup>

The silver iodide complex **1** (Scheme 2) was obtained by reaction of dimethylimidazolium iodide with silver(I) oxide, following the typical conditions for the synthesis of NHC-Ag<sup>I</sup> complexes.<sup>[15a,c,d]</sup> The virtual insolubility of **1** in common organic solvents such as THF and CH<sub>2</sub>Cl<sub>2</sub> supported the formation of a charge-separated complex. On the basis of elemental analysis data, **1** is best formulated as the ion pair [Ag(IMe)<sub>2</sub>]<sup>+</sup>(AgI<sub>2</sub>)<sup>-</sup>, in contrast with the formulation [Ag(IMe)<sub>2</sub>]<sub>2</sub>(Ag<sub>4</sub>I<sub>6</sub>), which was reported upon further recrystallisation from hot DMSO.<sup>[33]</sup> The formation of similar ion pairs, before and after an additional recrystallisation step, was also observed in the synthesis of [Ag(IMes)] (**2**).<sup>[31,34]</sup> Stirring a mixture of **1** with a slight excess (1.10 molar equiv.) of freshly filed europium or samarium metal afforded the highly air-sensitive divalent lanthanide complexes [Ln<sub>2</sub>(IMe)<sub>4</sub>] (Ln=Eu (**3**), Sm (**4**)) (Scheme 2). Although both starting materials were insoluble in THF, successful reaction could be evidenced by the formation of a fine black precipitate, presumably of elemental silver, along with orange-red and dark-green solutions in the case of europium and samarium,



**Scheme 2.** Synthesis of the lanthanide and alkaline-earth IMe complexes **3–7** by redox-transmetalation from **1**.

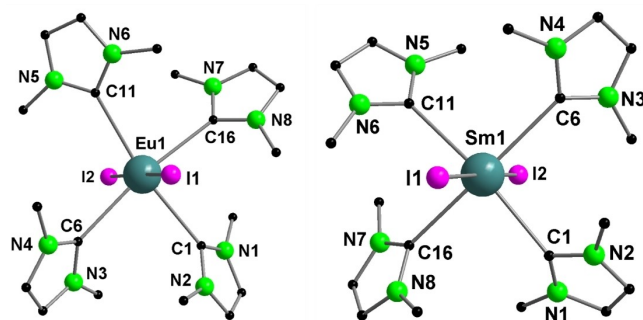


**Figure 1.** Molecular structures of **3** (left) and **4** (right) in the solid state. H atoms have been omitted for clarity. Selected bond lengths (Å) and angles [°] for **3**: Eu1–I1 3.3228(8), Eu1–I2 3.3072(8), Eu1–C1 2.811(8), Eu1–C6 2.799(9), Eu1–C11 2.815(8), Eu1–C16 2.811(8); I1–Eu1–I2 174.91(2), C1–Eu1–C11 170.6(3), C6–Eu1–C16 170.6(3); for **4**: Sm1–I1 3.236(2), Sm1–I2 3.254(2), Sm1–C1 2.74(3), Sm1–C6 2.85(2), Sm1–C11 2.79(3), Sm1–C16 2.83(3); I1–Sm1–I2 177.69(7), C1–Sm1–C11 168.2(9), C6–Sm1–C16 171.2(9). The asymmetric units of **3** and **4** contain three independent molecules with similar metrical data (see Table 1 and Supporting Information).

respectively. It is worth noting that highly coloured blue-green solutions are typical of  $\text{Sm}^{\text{II}}$  species, such as  $\text{SmI}_2$ , in ether solvents.<sup>[35]</sup> After decantation and careful filtration of the respective solutions, crystals of **3** and **4** suitable for X-ray diffraction studies were obtained upon concentration of the solutions by slow evaporation. The crystals were washed with a small amount of THF to remove the highly soluble  $[\text{LnI}_2(\text{THF})_n]$  complex that is presumably formed as a by-product. The molecular structures of **3** and **4** in the solid state (Figure 1) revealed isomorphous complexes that crystallised in the orthorhombic space group *Iba2* with three independent molecules in the asymmetric unit.

In these tetra-NHC adducts of  $\text{LnI}_2$ , the divalent lanthanide centre is lying in an almost ideal octahedral coordination geometry. The two iodides are located axially, *trans* to each other, forming I–M–I angles in the range 172.20(2)–178.18(2)° and with a mean value of ca. 175°, taking into account all the independent molecules in the asymmetric unit (see Table 1). The  $\text{Ln}^{\text{II}}\text{-C}^{\text{NHC}}$  bond lengths (2.73(3)–2.871(8) Å, with an average of ca. 2.80 Å) are in line with the distances reported for  $\text{Eu}^{\text{II}}$  and  $\text{Sm}^{\text{II}}$  NHC complexes.<sup>[31,36]</sup> Overall and within experimental error, **3** and **4** are isomorphous (identical metrical data, Table 1), which is consistent with the almost identical ionic radii of hexacoordinated  $\text{Eu}^{\text{II}}$  and  $\text{Sm}^{\text{II}}$  metal centres (ca. 1.17 Å).<sup>[37]</sup> It is worth noting that **3** is only the second example of a  $\text{Eu}^{\text{II}}$ -NHC complex, the other example corresponding to  $[\text{EuI}_2(\text{IMes})(\text{THF})_3]$ , described in our previous communication.<sup>[31]</sup> In the solid-state structures of **3** and **4**, an approximate, non-crystallographically imposed  $D_4$  symmetry is observed, with the NHC ligands arranged in a propeller-like fashion. The NHC rings are not coplanar with the idealised  $\text{MC}^{\text{NHC}}_4$  plane but form, with respect to the latter, an average torsion angle  $\theta_{\text{torsion}} = 44^\circ$  (Figure 2). Such a torsion angle may allow to minimise the steric repulsion of the methyl NHC wingtip substituents both with each other (maximum repulsion for  $\theta_{\text{torsion}} = 0^\circ$ ) and with the iodide ligands (maximum repulsion for  $\theta_{\text{torsion}} = 90^\circ$ ).<sup>[38]</sup> As a result, the molecule presents axial chirality or helicity,<sup>[39]</sup> the two possible enantiomers being depicted in Figure 3. It should however be stressed that **3** and **4** are obtained as racemic mixtures, which can be explained by the presence of symmetry operations of the second kind, namely glide planes, in the non-centrosymmetric achiral space group *Iba2*.<sup>[40]</sup> Consequently, within the complete unit cell, each motif is accompanied by its mirror

**Table 1.** Comparison of selected bond lengths (Å) and angles (deg) for complexes **3–10**.<sup>[a]</sup>

Compound general formula	<b>3</b> (Eu) <sup>[c]</sup> [ $\text{M}_2(\text{IME})_4$ ]	<b>4</b> (Sm) <sup>[c]</sup> [ $\text{M}_2(\text{IME})_4$ ]	<b>5</b> (Yb)	<b>6</b> (Ca) [ $\text{M}_2(\text{IME})_2(\text{THF})_2$ ]	<b>7</b> (Sr)	<b>8</b> (Sr)	<b>9</b> (Eu) <sup>[d]</sup> [ $\text{M}_2(\text{IMes})(\text{THF})_3$ ]	<b>10</b> (Yb) <sup>[d]</sup>
ionic radius <sup>[b]</sup>	1.17	1.17	1.02	1.00	1.18	1.18	1.17	1.02
M–I <sub>av.</sub>	3.27 ± 0.04	3.27 ± 0.04	3.137 ± 0.002	3.159 ± 0.003	3.266 ± 0.006	3.237 ± 0.012	3.218 ± 0.004	3.111 ± 0.005
M–O <sub>av.</sub>	–	–	2.436 ± 0.008	2.393 ± 0.015	2.53 ± 0.5	2.551 ± 0.012	2.560 ± 0.013	2.46 ± 0.02
M–C <sup>NHC</sup> <sub>av.</sub>	2.80 ± 0.03	2.80 ± 0.03	2.61 ± 0.02	2.61 ± 0.02	2.754 ± 0.012	2.779(4)	2.749(6)	2.650(3)
I–M–I	175 ± 3	175 ± 3	176.67(4)	176.98(6)	177.60(5)	177.26(2)	177.01(2)	177.46(1)
$\theta_{\text{torsion}}$	44 ± 4	44 ± 4	40 ± 8	40 ± 7	41 ± 6	–	–	–
$\theta_{\text{pitch}}$	9.4 ± 5.7	8.9 ± 6.0	3.9 ± 3.4	5.7 ± 3.1	3.8 ± 2.4	2.3	2.7	1.9
$\theta_{\text{yaw}}$	1.8 ± 1.1	1.7 ± 1.1	2.7 ± 0.5	2.1 ± 0.2	1.3 ± 1.7	0.3	0.05	0.2

[a] The ± values correspond to the standard deviations from the mean values. [b] Ionic radii (Å) for the divalent six-coordinate metal centres, taken from Ref. [37a] (for Sm(II), the same value as for Eu(II) was taken). [c] Presence of three independent molecules in the asymmetric unit. [d] Taken from Ref. [31].

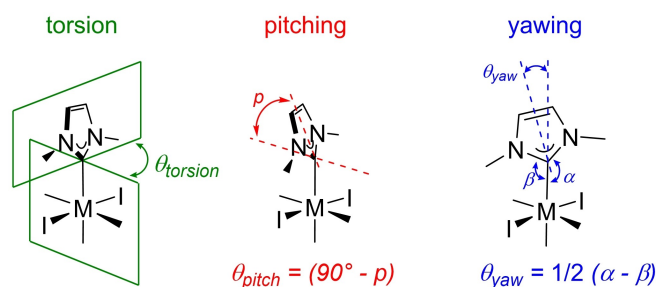


**Figure 2.** Schematic representation of the torsion angle between the NHC ring and the  $MC^{NHC}_4$  coordination plane (left), the pitch angle corresponding to out-of-plane tilting (middle) and the yaw angle describing in-plane tilting of the coordinated NHC ligand (right).

image. Moreover, the two possible enantiomers of  $[LnI_2(IMe)_4]$  (Figure 3) are present in the asymmetric units of **3** and **4** (which feature three independent molecules, see Supporting Information for more details). Tetra-NHC arrangements featuring monodentate NHC ligands have, so far, not been reported with lanthanide metal centres but have been mostly restricted to mid-to-late TMs, especially group 7 (Tc, Re),<sup>[41]</sup> group 8 (Fe,<sup>[42]</sup> Ru<sup>[43]</sup>) and group 9 (Co,<sup>[44]</sup> Rh<sup>[45]</sup>) metals. In addition, very rare examples of similar tetra-NHC complexes of molybdenum<sup>[38]</sup> and aluminium<sup>[46]</sup> have been reported.

A close inspection of the solid-state structures of **3** and **4** revealed further distortions of the coordinated IMe ligands from the idealised and symmetrical trigonal planar coordination geometry at the  $C^{NHC}$  atoms. Such deviations can be described in terms of pitch and yaw angles,<sup>[47]</sup> corresponding to out-of-plane and in-plane tilting of the NHC ligands, respectively, as depicted in Figure 2. The extent of the pitching and yawing distortions was found similar in **3** and **4** (Table 1) with an average yaw angle of ca.  $1.8^\circ$  (with values ranging from  $0.1$  to  $4.2^\circ$ ) and pitch angle of ca.  $9^\circ$  (with values spanning a much larger range of angles, from  $2.1$  to  $20.6^\circ$ ). The largest observed deviations,  $\theta_{pitch} = 20.6^\circ$  and  $\theta_{yaw} = 4.2^\circ$ , are quite remarkable; although slight geometrical distortions ( $\theta_{pitch}$  and  $\theta_{yaw}$  below  $10^\circ$ ) are common among TM-NHC complexes,<sup>[48]</sup> they are usually much more pronounced in the case of main-group and f-block elements,<sup>[36a,b,49]</sup> especially when using chelating functionalised NHC ligands.<sup>[4a,50]</sup>

When bulky NHC ligands are used, intramolecular repulsive interactions have been found as a major contributing factor for in-plane (yawing) and out-of-plane (pitching) tilting of the NHC

ligands.<sup>[48]</sup> However, the small size of the IMe ligand and the large distribution of pitching angles in **3** and **4** suggest that the observed distortions do not originate from intramolecular steric repulsion. In the case of gallium(I) bis-NHC complexes, secondary attractive interactions involving an unusual form of  $\sigma$ -back-donation from the filled gallium(I) s-type lone-pair to the vacant p-type orbital of the NHC ligand was found to account for the high pitching angles.<sup>[49e]</sup> However, in the  $Eu^{II}$  and  $Sm^{II}$  complexes **3** and **4**, the metal electronic configuration  $[Xe]4f^n$  ( $n=6$  and  $7$ , respectively) does not feature any filled  $6s$  orbital to engage in such a  $\sigma$ -back-bonding interaction. Another type of electronic back-donation from the lone pairs of the ligands located in *cis* position, rather than from the metal itself, to the NHC empty p-orbital has also been suggested in the case of high-valent  $d^0$  metal ( $V^V$ ,  $Nb^V$ ) complexes,<sup>[51]</sup> but such interactions were found negligible,<sup>[52]</sup> especially in the case of NHC adducts of samarium(III) chloride.<sup>[53]</sup> Therefore, intramolecular attractive interactions may not be either the origin of the distortions displayed in **3** and **4**. Careful analysis of the crystal packing in the corresponding X-ray structures revealed short contact interactions between the backbones of the most tilted NHC rings and those of adjacent  $[LnI_2(IMe)_4]$  molecules, suggesting that the high pitching and yawing angles arises from *intermolecular* packing effects. The optimised calculated structure of **4** in the gas phase (see Supporting Information for details) does not reproduce these distortions, which further supports solid-state effects (packing forces influencing intermolecular interactions) as the origins of the bending of the NHC ligands.

The very poor solubility of **3** and **4** in suitable solvents (e.g. toluene, THF), which seems to be typical for complexes of the type  $[MX_2(IMe)_4]$  ( $X$ =halide or hydride),<sup>[43e,f]</sup> and the paramagnetic nature of the complexes precluded analysis by NMR methods. In contrast, IR spectroscopy has proved to be a useful probe to investigate the coordination of the IMe ligand to paramagnetic lanthanide metal centres.<sup>[49a]</sup> In the IR spectra of **3** and **4** (see Supporting Information, Figures S11–12), an intense absorption band was observed in the range  $1574$ – $1575\text{ cm}^{-1}$  and is associated with the  $\nu(C=N)$  stretching vibration of the coordinated NHC ligand.

The same redox-transmetalation procedure with metallic ytterbium afforded the highly air-sensitive  $Yb^{II}$  complex  $[YbI_2(IMe)_2(THF)_2]$  (**5**) (Scheme 2), which was isolated in 45% yield as red crystals suitable for X-ray diffraction studies. The X-ray structure of **5** (Figure 4) displayed a slightly distorted octahedral coordination geometry around the  $Yb^{II}$  metal centre

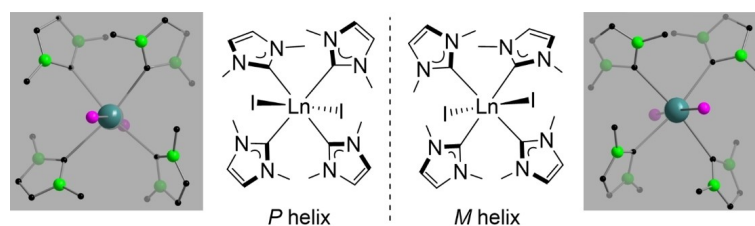


**Figure 3.** Representation of the two enantiomers of  $[LnI_2(IMe)_4]$  with in grey the idealised  $MC^{NHC}_4$  coordination plane.

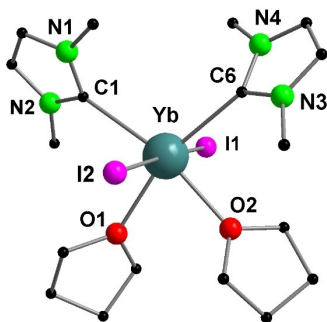


**Figure 4.** Molecular structure of **5** in the solid state. H atoms have been omitted for clarity. Selected bond lengths (Å) and angles [°]: Yb–I1 3.1358(13), Yb–I2 3.1380(13), Yb–O1 2.442(10), Yb–O2 2.430(10), Yb–C1 2.626(14), Yb–C6 2.603(14); I1–Yb–I2 176.67(4), O1–Yb–C6 163.1(4), O2–Yb–C1 167.1(4).

with two axial and mutually *trans* iodides forming an I–Yb–I angle of 176.67(4)°. The equatorial coordination plane is composed of two IMe and two THF ligands in a *cis* arrangement, resulting in an overall  $C_2$ -symmetric complex in the solid state. The Yb–C<sup>NHC</sup> bond distances (2.603(14)–2.626(14) Å) are within the typical range for Yb<sup>II</sup>-NHC complexes (from 2.552(4) to 2.710(5) Å).<sup>[31,36c,d,54]</sup> The Yb–I separation in **5** is ca. 0.13 Å shorter than that in **3** and **4**, which is consistent with the contraction of ca. 0.15 Å in the ionic radius from Sm<sup>II</sup> to Yb<sup>II</sup> (Table 1).

Contrary to **3** and **4**, the Yb<sup>II</sup> complex **5** crystallised in the monoclinic centrosymmetric space group  $P2_1/n$  and does not exhibit pronounced pitching or yawing angles (Table 1), which further supports packing effects as the main contributing factor to the distortions observed in the former complexes. The NHC rings in **5** are forming an angle of ca. 40° with respect to the C<sup>NHC</sup>O<sub>2</sub> equatorial coordination plane, resulting in a chiral helical arrangement. However, both enantiomers are present in the unit cell and related by the crystallographic inversion centre of  $P2_1/n$ , leading to an overall racemic mixture.<sup>[40b]</sup>

In contrast to **3** and **4**, the Yb<sup>II</sup> complex **5** is diamagnetic and presents an increased solubility in THF, which allowed characterisation by NMR spectroscopy. In its <sup>1</sup>H NMR spectrum, the methyl NHC wingtip substituents gave rise to a singlet at δ 3.90 ppm. Unfortunately, the coordinated C<sup>NHC</sup> resonance could not be detected in the <sup>13</sup>C{<sup>1</sup>H} NMR spectrum. An intense absorption band was observed at 1573 cm<sup>-1</sup> in the IR spectrum (see Supporting Information, Figure S13), confirming coordination of the IMe ligand.<sup>[49a]</sup>

Although identical reaction conditions were used for the synthesis of all Ln<sup>II</sup>-IMe complexes, the bis-NHC adduct **5** was exclusively obtained in the case of Yb<sup>II</sup> while tetra-NHC arrangements were isolated with Sm<sup>II</sup> and Eu<sup>II</sup> metal centres. Steric and electronic considerations may be invoked to rationalise this different coordination behaviour. The smaller ionic radius of the Yb<sup>2+</sup> ion (Table 1) may result in an increased steric pressure and higher charge density at the metal centre, favouring coordination of the relatively “harder” (in the sense of Pearson’s HSAB

concept)<sup>[55]</sup> and slightly less sterically encumbered THF ligand (see below for an additional discussion).

### Synthesis of divalent alkaline earth IMe complexes

With the successful synthesis of Ln<sup>II</sup> IMe complexes by redox-transmetalation, we were interested to evaluate whether the same procedure would also be applicable to access heavier divalent alkaline-earth NHC complexes. Indeed, the corresponding metals are highly reducing, with redox potentials associated with the M<sup>2+</sup>/M<sup>0</sup> couples (–2.87 for Ca and –2.90 V for Sr) similar to the values for Eu, Yb and Sm (–2.81, –2.76 and –2.68 V, respectively).<sup>[56]</sup> In addition, the ionic radii of the Eu<sup>2+</sup>, Sm<sup>2+</sup> and Sr<sup>2+</sup> cations are very close (1.17–1.18 Å for six-coordinate metal centres), as are those of the Yb<sup>2+</sup> and Ca<sup>2+</sup> ions (1.02 and 1.00 Å, respectively, for six-coordinate metal centres).<sup>[37a]</sup> Because of the similar sizes of divalent lanthanide and heavier alkaline-earth metal centres and their high electro-positive character, strong similarities in their coordination chemistry have been observed.<sup>[36d,37b,57]</sup> The bonding of these oxophilic M<sup>2+</sup> ions with coordinating ligand is mainly governed by electrostatic and steric factors.<sup>[58]</sup>

Reaction of **1** with calcium and strontium metal afforded, after crystallisation, the divalent alkaline-earth complexes [M(IMe)<sub>2</sub>(THF)<sub>2</sub>] (M = Ca (**6**), Sr (**7**)) in moderate isolated yields (48–71%) (Scheme 1) and the complexes were characterised by IR and NMR spectroscopy. In their IR spectra, a strong absorption band is observed at ca. 1573 cm<sup>-1</sup> (see Supporting Information, Figures S14–15), consistent with IMe coordination.<sup>[49a]</sup> The NMR spectra of **6** and **7** confirmed the presence of coordinated THF molecules, although the relative IMe vs. THF integrations in **7** indicate partial decoordination of THF upon drying the complex under vacuum.

The alkaline-earth complexes **6** and **7** are isomorphous with the Yb<sup>II</sup> complex **5**, crystallising in the same monoclinic space group  $P2_1/n$ . Analysis of the X-ray structures of **6** and **7** (Figure 5) revealed slightly distorted octahedral coordination

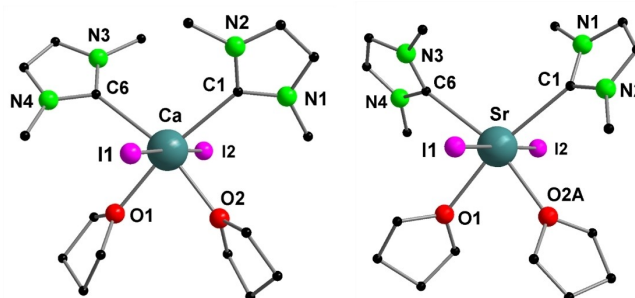
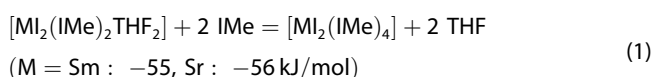


**Figure 5.** Molecular structures of **6** (left) and **7** (right) in the solid state. H atoms have been omitted and only one disordered position for the one THF ligand in **7** has been depicted for clarity. Selected bond lengths (Å) and angles [°] for **6**: Ca–I1 3.157(2), Ca–I2 3.161(2), Ca–O1 2.382(6), Ca–O2 2.403(6), Ca–C1 2.597(8), Ca–C6 2.632(8); I1–Ca–I2 176.98(6), O1–Ca–C1 169.4(2), O2–Ca–C6 165.2(3); for **7**: Sr–I1 3.270(2), Sr–I2 3.262(2), Sr–O1 2.528(10), Sr–C1 2.762(13), Sr–C6 2.745(12), Sr–O2A 2.49(4); I1–Sr–I2 177.60(5), O1–Sr–C1 167.7(3), O2A–Sr–C6 164(3).

geometries around the metal centres with two mutually *trans* iodides in an almost perfect linear arrangement (I–M–I angles in the range of 176.98(6)–177.60(5)°). The overall metrical data in the Ca<sup>II</sup> complex **6** are similar to those in the isostructural Yb<sup>II</sup> complex **5** (Table 1) with an average M–C<sup>NHC</sup> bond length of 2.61 Å, which reflects the similar ionic radii of hexacoordinated Ca<sup>2+</sup> and Yb<sup>2+</sup> ions.<sup>[37a]</sup> In the case of the Sr<sup>II</sup> complex **7**, the average Sr–C<sup>NHC</sup> bond length (2.754 Å) is ca. 0.14 Å longer, consistent with the larger ionic radius of Sr<sup>2+</sup> (Table 1). Although the ionic radii of hexacoordinated Eu<sup>2+</sup>, Sm<sup>2+</sup> and Sr<sup>2+</sup> ions are very close,<sup>[37a]</sup> their complexes with the IMe ligand are not isostructural: the divalent lanthanide IMe complexes **3** and **4** adopt a tetra-NHC arrangement while the Sr<sup>II</sup> complex **7** was exclusively isolated as a bis-NHC adduct under similar experimental conditions. This discrepancy indicates that mere hard/soft considerations based on ionic radius differences cannot solely explain the selectivity in the formation of bis- or tetra-NHC complexes. Interestingly, computational studies on the nature of the metal-ligand interaction in [Sm(C<sub>5</sub>Me<sub>5</sub>)<sub>2</sub>] and [Sr(C<sub>5</sub>Me<sub>5</sub>)<sub>2</sub>] by Clavaguéra, Nief and co-workers revealed an increased electronic charge at the metal centre in the latter complex, supporting a more ionic interaction in the case of strontium in comparison to samarium.<sup>[59]</sup> A corollary is that Sm<sup>II</sup>-ligand interactions may in some cases present a partially covalent character.

Therefore, dispersion corrected<sup>[60]</sup> RI-DFT calculations were performed using the BP-86 functional (see Table S2 in the Supporting Information) to investigate the bonding properties in the different [MI<sub>2</sub>(IMe)<sub>4</sub>] and [MI<sub>2</sub>(IMe)<sub>2</sub>THF<sub>2</sub>] molecules and try to rationalise the selective formation of the tetra- and bis-NHC complexes.<sup>[61]</sup> Within the two series of isostructural complexes, we focussed on the comparison of the Sr<sup>II</sup> and Sm<sup>II</sup> compounds; the theoretical structural results are in very good agreement with the experimental values. The basis sets were of def2-SV(P) quality for all atoms as given in the program package TURBOMOLE.<sup>[62]</sup> For iodine, samarium and strontium effective core potentials (ecp) of 46, 52 and 28 core electrons were used.

The calculated molecules are of symmetry *D*<sub>4</sub> ([MI<sub>2</sub>(IMe)<sub>4</sub>] with M=Sm, **4**, and the hypothetical complex with M=Sr, **7'**) and *C*<sub>2</sub> ([MI<sub>2</sub>(IMe)<sub>2</sub>THF<sub>2</sub>] with M=Sr, **7**, and the hypothetical complex with M=Sm, **4'**), respectively. A good overview on the bonding situation is obtained from an energetic comparison of the compounds. The formation of the respective tetra-NHC adduct from the bis-NHC adduct according to Equation (1) indicates a slightly stronger bond of the IMe ligand compared to THF.



The theoretical formation of [MI<sub>2</sub>(IMe)<sub>4</sub>] starting from the uncoordinated diiodides and IMe according to Equation (2) results in a bond dissociation energy of 147 and 148 kJ/mol for the Sm-IMe and the Sr-IMe bond, respectively. These values give a strong indication that bonding in **4** and hypothetical **7'** are of comparable character.

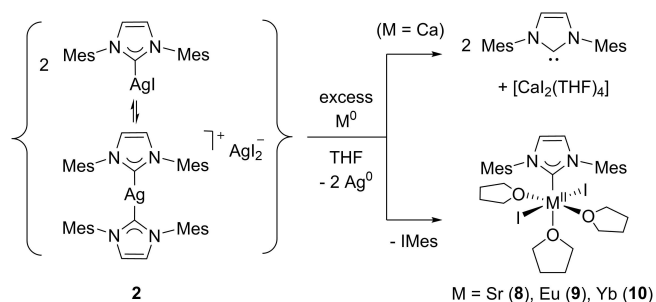


To evaluate the partial charges of the atoms and the extent of covalency of the M–C bonds, population analyses based on occupation numbers were performed according to the method of Ahlrichs and Heinzmann.<sup>[63]</sup> In contrast to the not-negligible covalent bonding in samarocene [SmCp\*<sub>2</sub>] (Cp\* = η<sup>5</sup>-C<sub>5</sub>Me<sub>5</sub>) compared to that in [SrCp\*<sub>2</sub>] found in the work by Clavaguéra, Nief and co-workers,<sup>[59]</sup> predominantly ionic bonding is found for the tetra-NHC complexes **4** and **7'**, or the bis-NHC adducts **4'** and **7**. Strong indication is given by the partial charges at the metal centres, which are almost of the same size as for the uncoordinated molecules SmI<sub>2</sub> and SrI<sub>2</sub>. In **7** and **4'**, a stronger donor property of THF is found compared to IMe, evident from the total sum of partial atomic charges of the ligands. This effect increases polarization of the M–C bond, but not to an extent of a change of the qualitative bonding scheme within the bis-NHC and tetra-NHC adducts. The shared electron number (SEN) of the M–C bonds in all molecules under discussion is calculated to be less than 0.35 giving hint of only minor covalent bonding.

Moreover, as an even more convincing proof, the energies of the theoretically calculated metal-carbon stretching vibrations in these molecules represent another very sensitive measure of their bonding forces that can directly be compared to each other. Since all M–C stretching vibrations for all compounds discussed here are in the close range between 317 and 320 cm<sup>–1</sup>, it can be convincingly assumed that the bonding in these compounds is of comparable ionic character. In summary, calculations show that tetra-NHC arrangements should be favoured for both Sm and Sr, at least in the gas phase. However, the energy differences between both species are moderate and in THF solution the equilibrium is influenced by the high concentration of the solvent. In THF, which is the only solvent we found as suitable for NMR studies, we could not detect any dynamic processes - maybe because they are too fast. ESI-MS measurements out of solution showed only fragments. For the product formation, it must be considered that also the crystallisation step shifts the equilibrium. Furthermore, different crystal packing forces in the solid state may influence the selective formation of the Sr<sup>II</sup> bis-NHC complex **7**, considering that **4** and **7** crystallise in different crystal systems.

### Synthesis of divalent alkaline earth IMes complexes

To investigate the generality of the redox-transmetalation procedure using alkaline-earth metals, the reaction of [AgI(IMes)] (**2**) with excess of freshly filed strontium metal was performed under similar reaction conditions, as described above (Scheme 3). It should be noted that the silver complex **2** exists as an equilibrium mixture between two structural isomers, the heteroleptic [AgI(IMes)] and the homoleptic ion pair [Ag(IMes)<sub>2</sub>]<sup>+</sup>(AgI<sub>2</sub>)<sup>–</sup>.<sup>[15a,64]</sup> After filtration of the insoluble black precipitate, slow evaporation of the solvent afforded



**Scheme 3.** Redox-transmetalation of **2** with alkaline-earth (Ca, Sr) metals and previously reported reaction with lanthanide metals (Eu, Yb).<sup>[31]</sup>

colourless crystals of  $[\text{SrI}_2(\text{IMes})(\text{THF})_3]$  (**8**) suitable for X-ray diffraction studies and isomorphous to the divalent lanthanide complexes  $[\text{LnI}_2(\text{IMes})(\text{THF})_3]$  ( $\text{Ln}=\text{Eu}$  (**9**) and  $\text{Yb}$ (**10**)),<sup>[31]</sup> all of them crystallising in the centrosymmetric orthorhombic space group *Pbca*.

Analysis of the crystal structure of **8** (Figure 6) revealed a slightly distorted octahedral coordination environment around the  $\text{Sr}^{2+}$  ion, the latter surrounded by one IMes ligand, three THF donors and two mutually *trans* iodides. The IMes complexes **8–10** feature negligible pitching and yawing distortions for the coordinated NHC ligand (Table 1). The  $\text{Sr}-\text{C}^{\text{NHC}}$  bond length of 2.779(4) Å is close to that in the  $\text{Eu}^{\text{II}}$  complex **9** (2.749(6) Å)<sup>[31]</sup> in line with the similar ionic radii of both metal centres. Similarly, the average  $\text{Sr}-\text{I}$  and  $\text{Eu}-\text{I}$  separations in **8** and **9**, ca. 3.24 and 3.22 Å, respectively, are very close. No obvious elongation of the  $\text{Sr}-\text{O}^{\text{THF}}$  bond distance in *trans* position relative to the NHC donor was observed. The  $^1\text{H}$  and  $^{13}\text{C}\{^1\text{H}\}$  NMR spectra of **8** in  $\text{C}_6\text{D}_6$  are similar to those of the isostructural and diamagnetic  $\text{Yb}^{\text{II}}$  complex **10** and, in both case, the  $\text{C}^{\text{NHC}}$  resonance could not be detected in the corresponding  $^{13}\text{C}\{^1\text{H}\}$  NMR spectra.<sup>[31]</sup>

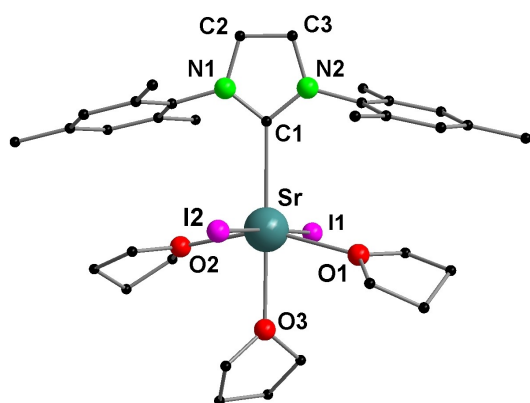


**Figure 6.** Molecular structure of **8** in the solid state. H atoms and non-coordinating solvent molecules have been omitted for clarity. Selected bond lengths (Å) and angles [°]:  $\text{Sr}-\text{I}1$  3.2284(5),  $\text{Sr}-\text{I}2$  3.2458(4),  $\text{Sr}-\text{O}1$  2.549(3),  $\text{Sr}-\text{O}2$  2.541(3),  $\text{Sr}-\text{O}3$  2.564(3),  $\text{Sr}-\text{C}1$  2.779(4);  $\text{I}1-\text{Sr}-\text{I}2$  177.258(15),  $\text{O}3-\text{Sr}-\text{C}1$  177.12(11),  $\text{O}1-\text{Sr}-\text{O}2$  154.46(10).

Interestingly, the redox-transmetalation reaction of **2** with elemental calcium did not result in the formation of the  $\text{Ca}^{\text{II}}$  analogue of **8–10** (Scheme 3). Instead,  $[\text{Ca}_2(\text{THF})_4]$  was isolated from the reaction mixture, indicating preferential coordination with the alkaline-earth metal centre of the “harder” THF donors compared to the “softer” IMes ligand, which is also consistent with the formation of the bis-NHC  $\text{Sr}^{\text{II}}$  adduct **7**.

Finally, synthesis of the  $\text{Sm}^{\text{II}}$  analogue of **8–10** was attempted by reaction of **2** with samarium metal following the same procedure as described above. Although a deep blue solution was initially formed, supporting formation of  $\text{Sm}^{\text{II}}$  species in solution,<sup>[35]</sup> the reaction mixture repeatedly evolved into an intractable brown oil at room temperature even in a sealed glass ampoule. This behaviour is probably linked to the high reductive character of  $\text{Sm}^{\text{II}}$  and the labile coordination of the relatively bulky IMes ligand, in contrast with stronger coordination of the smaller IMe ligand in **4**. It should also be noted that successful formation of **3–10** was only possible using silver *iodide* NHC complexes as redox-transmetalation partners. Attempts to perform the same reactions with chloride analogues of **1** and **2** or with  $[\text{Ag}(\text{NHC})_2](\text{BPh}_4)$  ( $\text{NHC}=\text{IME}$ , IMes) did not lead to any conversion of the starting materials, revealing the importance of the nature of the halide anion in these redox-transmetalation reactions. The lack of reactivity in the absence of iodide counter anion, although surprising, may be linked to the higher size and facility of exchange of iodide compared to chloride anions, which may facilitate the electron transfer. In turn, the choice of the anion may also tune the reduction potential of the  $\text{NHC}-\text{Ag}(\text{I})$  complex.

## Conclusion

Divalent lanthanide ( $\text{Ln}=\text{Sm}$ ,  $\text{Eu}$ ,  $\text{Yb}$ ) and alkaline-earth ( $\text{M}=\text{Ca}$ ,  $\text{Sr}$ ) complexes supported by NHC ligands have been successfully obtained by using a redox-transmetalation strategy involving reaction of the corresponding zerovalent metals with air-stable  $\text{Ag}^{\text{I}}$ -NHC complexes. Different series of isostructural complexes were isolated, which allowed a precise comparison of the NHC bonding in these complexes to be drawn. Preferential formation of the tetra-NHC complexes  $[\text{LnI}_2(\text{IME})_4]$  ( $\text{Ln}=\text{Eu}$  (**3**),  $\text{Sm}$  (**4**)) was observed in the case of  $\text{Eu}^{\text{II}}$  and  $\text{Sm}^{\text{II}}$ , in contrast to the formation of  $[\text{SrI}_2(\text{IME})_2(\text{THF})_2]$  (**7**), despite the similar sizes or hexacoordinated  $\text{Eu}^{\text{II}}$ ,  $\text{Sm}^{\text{II}}$  and  $\text{Sr}^{\text{II}}$  ions. Similarly, preferential coordination of the IMes ligand to  $\text{Yb}^{\text{II}}$  in comparison to  $\text{Ca}^{\text{II}}$  was observed. Although DFT calculations support the easy formation of the tetra-NHC adducts for both  $\text{Sm}^{\text{II}}$  and  $\text{Sr}^{\text{II}}$ , the coordination differences observed experimentally certainly arise from subtle energetic differences in the solid state (different packing forces for example).

The redox-transmetalation procedure highlighted in this article may find applications in the synthesis of other NHC complexes of f-block elements or highly electropositive metal centres, in which the usual, non-redox transmetalation methodology from  $\text{Ag}^{\text{I}}$ -NHC complexes fails to proceed.

## Experimental Section

See the Supporting Information for the synthesis and characterisation of all compounds, the NMR and IR spectra, as well as X-ray crystallography and DFT calculation details.

**Crystallographic data:** Deposition Numbers 2086921 (for **3**), 2086922 (for **4**), 2086923 (for **5**), 2086924 (for **6**), 2086925 (for **7**), and 2086926 (for **8**-THF) contain the supplementary crystallographic data for this paper. These data are provided free of charge by the joint Cambridge Crystallographic Data Centre and Fachinformationszentrum Karlsruhe Access Structures service [www.ccdc.cam.ac.uk/structures](http://www.ccdc.cam.ac.uk/structures).

## Acknowledgements

This work is supported by the German Federal Ministry of Education and Research (BMBF) under Contracts 02NUK059F. The authors acknowledge computational support by the state of Baden-Württemberg through bwHPC and the Deutsche Forschungsgemeinschaft (DFG) through grant No INST 40/467-1 FUGG. T.S. thanks the Alexander von Humboldt Foundation for a postdoctoral fellowship. Open access funding enabled and organized by Projekt DEAL.

## Conflict of Interest

The authors declare no conflict of interest.

**Keywords:** alkaline earth metals · carbene ligands · divalent lanthanides · metal-ligand interactions · redox-transmetalation

- [1] a) A. J. Arduengo, R. L. Harlow, M. Kline, *J. Am. Chem. Soc.* **1991**, *113*, 361–363; b) F. E. Hahn, M. C. Jahnke, *Angew. Chem. Int. Ed.* **2008**, *47*, 3122–3172; *Angew. Chem.* **2008**, *120*, 3166–3216.
- [2] a) D. Pugh, A. A. Danopoulos, *Coord. Chem. Rev.* **2007**, *251*, 610–641; b) S. Bellemin-Lapponnaz, S. Dagorne, *Chem. Rev.* **2014**, *114*, 8747–8774; c) J. Cheng, L. Wang, P. Wang, L. Deng, *Chem. Rev.* **2018**, *118*, 9930–9987; d) A. A. Danopoulos, T. Simler, P. Braunstein, *Chem. Rev.* **2019**, *119*, 3730–3961; e) C. Romain, S. Bellemin-Lapponnaz, S. Dagorne, *Coord. Chem. Rev.* **2020**, *422*, 213411.
- [3] a) C. Fliedel, G. Schnee, T. Avilés, S. Dagorne, *Coord. Chem. Rev.* **2014**, *275*, 63–86; b) V. Nesterov, D. Reiter, P. Bag, P. Frisch, R. Holzner, A. Porzelt, S. Inoue, *Chem. Rev.* **2018**, *118*, 9678–9842; c) A. Doddi, M. Peters, M. Tamm, *Chem. Rev.* **2019**, *119*, 6994–7112; d) B. Borthakur, B. Ghosh, A. K. Phukan, *Polyhedron* **2021**, *197*, 115049.
- [4] a) P. L. Arnold, S. T. Liddle, *Chem. Commun.* **2006**, 3959–3971; b) P. L. Arnold, I. J. Casely, *Chem. Rev.* **2009**, *109*, 3599–3611; c) Y. Pan, X. Jiang, Y.-M. So, C. T. To, G. He, *Catalysts* **2020**, *10*, 71.
- [5] E. Peris, *Chem. Rev.* **2018**, *118*, 9988–10031.
- [6] a) W. A. Herrmann, *Angew. Chem. Int. Ed.* **2002**, *41*, 1290–1309; *Angew. Chem.* **2002**, *114*, 1342–1363; b) S. Díez-González, N. Marion, S. P. Nolan, *Chem. Rev.* **2009**, *109*, 3612–3676; c) G. C. Vougioukalakis, R. H. Grubbs, *Chem. Rev.* **2010**, *110*, 1746–1787; d) Á. Vivancos, C. Segarra, M. Albrecht, *Chem. Rev.* **2018**, *118*, 9493–9586; e) M. Iglesias, L. A. Oro, *Chem. Soc. Rev.* **2018**, *47*, 2772–2808; f) Q. Liang, D. Song, *Chem. Soc. Rev.* **2020**, *49*, 1209–1232; g) Q. Zhao, G. Meng, S. P. Nolan, M. Szostak, *Chem. Rev.* **2020**, *120*, 1981–2048.
- [7] a) R. Visbal, M. C. Gimeno, *Chem. Soc. Rev.* **2014**, *43*, 3551–3574; b) W. Liu, R. Gust, *Coord. Chem. Rev.* **2016**, *329*, 191–213; c) N. A. Johnson, M. R. Southerland, W. J. Youngs, *Molecules* **2017**, *22*, 1263; d) C. A. Smith, M. R. Narouz, P. A. Lummis, I. Singh, A. Nazemi, C.-H. Li, C. M. Crudden, *Chem. Rev.* **2019**, *119*, 4986–5056; e) S. Y. Hussaini, R. A. Haque, M. R. Razali, *J. Organomet. Chem.* **2019**, *882*, 96–111.
- [8] a) T. Scattolin, S. P. Nolan, *Trends Chem.* **2020**, *2*, 721–736; b) E. A. Martynova, N. V. Tzouras, G. Pisanò, C. S. J. Cazin, S. P. Nolan, *Chem. Commun.* **2021**, 57, 3836–3856.
- [9] A. J. Arduengo, H. V. R. Dias, R. L. Harlow, M. Kline, *J. Am. Chem. Soc.* **1992**, *114*, 5530–5534.
- [10] a) W. A. Herrmann, M. Elison, J. Fischer, C. Köcher, G. R. J. Artus, *Angew. Chem. Int. Ed. Engl.* **1995**, *34*, 2371–2374; *Angew. Chem.* **1995**, *107*, 2602–2605; b) W. A. Herrmann, J. Schwarz, M. G. Gardiner, *Organometallics* **1999**, *18*, 4082–4089; c) E. Peris, J. A. Loch, J. Mata, R. H. Crabtree, *Chem. Commun.* **2001**, 201–202; d) H. Lebel, M. K. Janes, A. B. Charette, S. P. Nolan, *J. Am. Chem. Soc.* **2004**, *126*, 5046–5047.
- [11] a) F. E. Hahn, C. Holtgrewe, T. Pape, M. Martin, E. Sola, L. A. Oro, *Organometallics* **2005**, *24*, 2203–2209; b) H. Türkmen, T. Pape, F. E. Hahn, B. Çetinkaya, *Organometallics* **2008**, *27*, 571–575; c) H. Türkmen, T. Pape, F. E. Hahn, B. Çetinkaya, *Eur. J. Inorg. Chem.* **2008**, 5418–5423; d) M. V. Jiménez, J. Fernández-Tornos, J. J. Pérez-Torrente, F. J. Modrego, S. Winterle, C. Cunchillos, F. J. Lahoz, L. A. Oro, *Organometallics* **2011**, *30*, 5493–5508.
- [12] a) A. A. Danopoulos, N. Tsoareas, J. A. Wright, M. E. Light, *Organometallics* **2004**, *23*, 166–168; b) A. A. Danopoulos, J. A. Wright, W. B. Motherwell, S. Ellwood, *Organometallics* **2004**, *23*, 4807–4810; c) A. A. Danopoulos, P. Braunstein, N. Stylianides, M. Wesolek, *Organometallics* **2011**, *30*, 6514–6517; d) S. Meyer, C. M. Orben, S. Demeshko, S. Dechert, F. Meyer, *Organometallics* **2011**, *30*, 6692–6702; e) A. Raba, M. Cokoja, S. Ewald, K. Riener, E. Herdtweck, A. Pöthig, W. A. Herrmann, F. E. Kühn, *Organometallics* **2012**, *31*, 2793–2800; f) D. T. Weiss, M. R. Anneser, S. Haslinger, A. Pöthig, M. Cokoja, J.-M. Basset, F. E. Kühn, *Organometallics* **2015**, *34*, 5155–5166; g) T. Simler, P. Braunstein, A. A. Danopoulos, *Chem. Commun.* **2016**, 52, 2717–2720; h) T. Simler, S. Choua, A. A. Danopoulos, P. Braunstein, *Dalton Trans.* **2018**, *47*, 7888–7895.
- [13] a) A. A. Danopoulos, P. Cole, S. P. Downing, D. Pugh, *J. Organomet. Chem.* **2008**, *693*, 3369–3374; b) T. Simler, P. Braunstein, A. A. Danopoulos, *Dalton Trans.* **2016**, *45*, 5122–5139; c) T. Simler, K. Möbius, K. Müller, T. J. Feuerstein, M. T. Gamer, S. Lebedkin, M. M. Kappes, P. W. Roesky, *Organometallics* **2019**, *38*, 3649–3661.
- [14] a) A. M. Bryan, G. J. Long, F. Grandjean, P. P. Power, *Inorg. Chem.* **2013**, *52*, 12152–12160; b) D. L. J. Broere, I. Čorić, A. Brosnahan, P. L. Holland, *Inorg. Chem.* **2017**, *56*, 3140–3143.
- [15] a) H. M. J. Wang, I. J. B. Lin, *Organometallics* **1998**, *17*, 972–975; b) J. C. Garrison, W. J. Youngs, *Chem. Rev.* **2005**, *105*, 3978–4008; c) I. J. B. Lin, C. S. Vasam, *Coord. Chem. Rev.* **2007**, *251*, 642–670; d) J. C. Y. Lin, R. T. W. Huang, C. S. Lee, A. Bhattacharyya, W. S. Hwang, I. J. B. Lin, *Chem. Rev.* **2009**, *109*, 3561–3598.
- [16] a) D. J. Nielsen, K. J. Cavell, B. W. Skelton, A. H. White, *Inorg. Chim. Acta* **2003**, *352*, 143–150; b) D. Hollmann, A. R. Kennedy, M. D. Spicer, T. Rannial, J. A. C. Clyburne, C. D. Abernethy, *J. Organomet. Chem.* **2005**, *690*, 5346–5352; c) V. N. Mikhaylov, I. V. Kazakov, T. N. Parfeniuk, O. V. Khoroshilova, M. Scheer, A. Y. Timoshkin, I. A. Balova, *Dalton Trans.* **2021**, *50*, 2872–2879.
- [17] P. L. Arnold, A. C. Scarisbrick, *Organometallics* **2004**, *23*, 2519–2521.
- [18] E. Mas-Marzá, M. Sanaú, E. Peris, *Inorg. Chem.* **2005**, *44*, 9961–9967.
- [19] a) Z. Lu, S. A. Cramer, D. M. Jenkins, *Chem. Sci.* **2012**, *3*, 3081–3087; b) R. A. Haque, M. Z. Ghadheyab, S. Budagumpi, M. B. Khadeer Ahmed, A. M. S. Abdul Majid, *RSC Adv.* **2016**, *6*, 60407–60421.
- [20] B. Liu, Q. Xia, W. Chen, *Angew. Chem. Int. Ed.* **2009**, *48*, 5513–5516; *Angew. Chem.* **2009**, *121*, 5621–5624.
- [21] M. V. Baker, D. H. Brown, R. A. Haque, P. V. Simpson, B. W. Skelton, A. H. White, C. C. Williams, *Organometallics* **2009**, *28*, 3793–3803.
- [22] Z. Guo, R. Huo, Y. Q. Tan, V. Blair, G. B. Deacon, P. C. Junk, *Coord. Chem. Rev.* **2020**, *415*, 213232.
- [23] a) G. B. Deacon, A. J. Koplick, T. D. Tuong, *Polyhedron* **1982**, *1*, 423–424; b) G. B. Deacon, A. Koplick, T. Tuong, *Aust. J. Chem.* **1984**, *37*, 517–525; c) G. B. Deacon, C. M. Forsyth, *Organometallics* **2003**, *22*, 1349–1352; d) R. P. Kelly, T. D. M. Bell, R. P. Cox, D. P. Daniels, G. B. Deacon, F. Jaroschik, P. C. Junk, X. F. Le Goff, G. Lemercier, A. Martinez, J. Wang, D. Werner, *Organometallics* **2015**, *34*, 5624–5636.
- [24] a) B. Çetinkaya, P. B. Hitchcock, M. F. Lappert, R. G. Smith, *J. Chem. Soc. Chem. Commun.* **1992**, 932–934; b) C. N. de Bruin-Dickason, A. J. Boutland, D. Dange, G. B. Deacon, C. Jones, *Dalton Trans.* **2018**, *47*, 9512–9520.
- [25] L. Clark, G. B. Deacon, C. M. Forsyth, P. C. Junk, P. Mountford, J. P. Townley, *Dalton Trans.* **2010**, *39*, 6693–6704.
- [26] a) G. B. Deacon, E. E. Delbridge, B. W. Skelton, A. H. White, *Eur. J. Inorg. Chem.* **1998**, 543–545; b) S. Beaini, G. B. Deacon, E. E. Delbridge, P. C. Junk, B. W. Skelton, A. H. White, *Eur. J. Inorg. Chem.* **2008**, 4586–4596.



- [27] K. Krogh-Jespersen, M. D. Romanelli, J. H. Melman, T. J. Emge, J. G. Brennan, *Inorg. Chem.* **2010**, *49*, 552–560.
- [28] a) G. B. Deacon, W. D. Raverty, D. G. Vince, *J. Organomet. Chem.* **1977**, *135*, 103–114; b) G. B. Deacon, C. M. Forsyth, S. Nickel, *J. Organomet. Chem.* **2002**, *647*, 50–60.
- [29] S. Beaini, G. B. Deacon, M. Hilder, P. C. Junk, D. R. Turner, *Eur. J. Inorg. Chem.* **2006**, 3434–3441.
- [30] a) Z. Guo, V. Blair, G. B. Deacon, P. C. Junk, *Chem. Eur. J.* **2018**, *24*, 17464–17474; b) Z. Guo, J. Luu, V. Blair, G. B. Deacon, P. C. Junk, *Eur. J. Inorg. Chem.* **2019**, 1018–1029; c) Z. Guo, V. L. Blair, G. B. Deacon, P. C. Junk, *Dalton Trans.* **2020**, 49, 13588–13600.
- [31] T. Simler, T. J. Feuerstein, R. Yadav, M. T. Gamer, P. W. Roesky, *Chem. Commun.* **2019**, 55, 222–225.
- [32] V. M. Chernyshev, E. A. Denisova, D. B. Eremin, V. P. Ananikov, *Chem. Sci.* **2020**, *11*, 6957–6977.
- [33] W. Chen, F. Liu, *J. Organomet. Chem.* **2003**, *673*, 5–12.
- [34] P. de Frémont, N. M. Scott, E. D. Stevens, T. Rammil, O. C. Lightbody, C. L. B. Macdonald, J. A. C. Clyburne, C. D. Abernethy, S. P. Nolan, *Organometallics* **2005**, *24*, 6301–6309.
- [35] P. Girard, J. L. Namy, H. B. Kagan, *J. Am. Chem. Soc.* **1980**, *102*, 2693–2698.
- [36] a) A. J. Arduengo, M. Tamm, S. J. McLain, J. C. Calabrese, F. Davidson, W. J. Marshall, *J. Am. Chem. Soc.* **1994**, *116*, 7927–7928; b) M. Glanz, S. Dechert, H. Schumann, D. Wolff, J. Springer, *Z. Anorg. Allg. Chem.* **2000**, *626*, 2467–2477; c) A. Pindwal, A. Ellern, A. D. Sadow, *Organometallics* **2016**, *35*, 1674–1683; d) I. V. Lapshin, I. V. Basalov, K. A. Lyssenko, A. V. Cherkasov, A. A. Trifonov, *Chem. Eur. J.* **2019**, *25*, 459–463.
- [37] a) R. Shannon, *Acta Crystallogr., Sect. A: Cryst. Phys., Diff., Theor. Gen. Crystallogr.* **1976**, *32*, 751–767; b) M. D. Walter, G. Wolmershäuser, H. Sitzmann, *J. Am. Chem. Soc.* **2005**, *127*, 17494–17503.
- [38] Y. Ohki, K. Aoyagi, H. Seino, *Organometallics* **2015**, *34*, 3414–3420.
- [39] a) R. S. Cahn, C. Ingold, V. Prelog, *Angew. Chem. Int. Ed. Engl.* **1966**, *5*, 385–415; *Angew. Chem.* **1966**, *78*, 413–447; b) G. P. Moss, *Pure Appl. Chem.* **1996**, *68*, 2193–2222.
- [40] a) A. L. Thompson, D. J. Watkin, *Tetrahedron: Asymmetry* **2009**, *20*, 712–717; b) A. Linden, *Tetrahedron: Asymmetry* **2017**, *28*, 1314–1320.
- [41] a) H. Braband, T. I. Zahn, U. Abram, *Inorg. Chem.* **2003**, *42*, 6160–6162; b) T. I. Kückmann, U. Abram, *Inorg. Chem.* **2004**, *43*, 7068–7074; c) B. Royo, E. Herdtweck, Carlos C. Romão, *Eur. J. Inorg. Chem.* **2004**, 3305–3309; d) H. Braband, D. Przyrembel, U. Abram, *Z. Anorg. Allg. Chem.* **2006**, *632*, 779–785; e) M. Benz, B. Spingler, R. Alberto, H. Braband, *J. Am. Chem. Soc.* **2013**, *135*, 17566–17572.
- [42] Z. Ouyang, Y. Meng, J. Cheng, J. Xiao, S. Gao, L. Deng, *Organometallics* **2016**, *35*, 1361–1367.
- [43] a) P. B. Hitchcock, M. F. Lappert, P. L. Pye, *J. Chem. Soc. Chem. Commun.* **1976**, 644–646; b) P. B. Hitchcock, M. F. Lappert, P. L. Pye, *J. Chem. Soc. Dalton Trans.* **1978**, 826–836; c) S. Burling, L. J. L. Häller, E. Mas-Marzá, A. Moreno, S. A. Macgregor, M. F. Mahon, P. S. Pregosin, M. K. Whittlesey, *Chem. Eur. J.* **2009**, *15*, 10912–10923; d) R. Wolf, M. Plois, A. Hepp, *Eur. J. Inorg. Chem.* **2010**, 918–925; e) M. Würtemberger, T. Ott, C. Döring, T. Schaub, U. Radius, *Eur. J. Inorg. Chem.* **2011**, 405–415; f) M. K. Cybulski, D. McKay, S. A. Macgregor, M. F. Mahon, M. K. Whittlesey, *Angew. Chem. Int. Ed.* **2017**, *56*, 1515–1519; *Angew. Chem.* **2017**, *129*, 1537–1541.
- [44] Z. Mo, Y. Li, H. K. Lee, L. Deng, *Organometallics* **2011**, *30*, 4687–4694.
- [45] W. A. Herrmann, J. Schütz, G. D. Frey, E. Herdtweck, *Organometallics* **2006**, *25*, 2437–2448.
- [46] H. Schneider, A. Hock, R. Bertermann, U. Radius, *Chem. Eur. J.* **2017**, *23*, 12387–12398.
- [47] a) S. A. Mungur, S. T. Liddle, C. Wilson, M. J. Sarsfield, P. L. Arnold, *Chem. Commun.* **2004**, 2738–2739; b) C. H. Leung, C. D. Incarvito, R. H. Crabtree, *Organometallics* **2006**, *25*, 6099–6107.
- [48] J.-N. Luy, S. A. Hauser, A. B. Chaplin, R. Tonner, *Organometallics* **2015**, *34*, 5099–5112.
- [49] a) W. A. Herrmann, F. C. Munck, G. R. J. Artus, O. Runte, R. Anwänder, *Organometallics* **1997**, *16*, 682–688; b) W. Marco Boesveld, B. Gehrhus, P. B. Hitchcock, M. F. Lappert, P. von Ragué Schleyer, *Chem. Commun.* **1999**, 755–756; c) A. J. Arduengo, R. Krczyk, R. Schmutzler, W. Mahler, W. J. Marshall, *Z. Anorg. Allg. Chem.* **1999**, *625*, 1813–1817; d) H. Schumann, J. Gottfriedsen, M. Glanz, S. Dechert, J. Demtschuk, *J. Organomet. Chem.* **2001**, *617–618*, 588–600; e) A. Higelin, S. Keller, C. Göhringer, C. Jones, I. Krossing, *Angew. Chem. Int. Ed.* **2013**, *52*, 4941–4944; *Angew. Chem.* **2013**, *125*, 5041–5044.
- [50] a) M. Zhang, X. Ni, Z. Shen, *Organometallics* **2014**, *33*, 6861–6867; b) P. L. Arnold, R. W. F. Kerr, C. Weetman, S. R. Docherty, J. Rieb, F. L. Cruickshank, K. Wang, C. Jandl, M. W. McMullon, A. Pöthig, F. E. Kühn, A. D. Smith, *Chem. Sci.* **2018**, *9*, 8035–8045.
- [51] C. D. Abernethy, G. M. Codd, M. D. Spicer, M. K. Taylor, *J. Am. Chem. Soc.* **2003**, *125*, 1128–1129.
- [52] G. Ciancaleoni, L. Belpassi, F. Marchetti, *Inorg. Chem.* **2017**, *56*, 11266–11274.
- [53] a) L. Maron, D. Bourissou, *Organometallics* **2007**, *26*, 1100–1103; b) L. Maron, D. Bourissou, *Organometallics* **2009**, *28*, 3686–3690.
- [54] a) H. Schumann, M. Glanz, J. Winterfeld, H. Hemling, N. Kuhn, T. Kratz, *Angew. Chem. Int. Ed.* **1994**, *33*, 1733–1734; *Angew. Chem.* **1994**, *106*, 1829–1830; ; b) H. Schumann, M. Glanz, J. Winterfeld, H. Hemling, N. Kuhn, T. Kratz, *Chem. Ber.* **1994**, *127*, 2369–2372; c) G. M. Ferrence, A. J. Arduengo, A. Jockisch, H.-J. Kim, R. McDonald, J. Takats, *J. Alloys Compd.* **2006**, *418*, 184–188; d) W. Xie, H. Hu, C. Cui, *Angew. Chem. Int. Ed.* **2012**, *51*, 11141–11144; *Angew. Chem.* **2012**, *124*, 11303–11306; e) J. Yuan, H. Hu, C. Cui, *Chem. Eur. J.* **2016**, *22*, 5778–5785.
- [55] a) R. G. Pearson, *J. Am. Chem. Soc.* **1963**, *85*, 3533–3539; b) R. G. Pearson, *Inorg. Chim. Acta* **1995**, *240*, 93–98.
- [56] P. Vanýšek, “Electrochemical Series” in *CRC Handbook of Chemistry and Physics, 85<sup>th</sup> Edition* (Ed. D. R. Lide), CRC Press, Boca Raton, FL, **2004**, pp. 8–23 to 8–28.
- [57] a) K. Izod, W. Clegg, S. T. Liddle, *Organometallics* **2000**, *19*, 3640–3643; b) F. Weber, M. Schultz, C. D. Sofield, R. A. Andersen, *Organometallics* **2002**, *21*, 3139–3146; c) S. Harder, *Angew. Chem. Int. Ed.* **2004**, *43*, 2714–2718; *Angew. Chem.* **2004**, *116*, 2768–2773; d) T. K. Panda, A. Zulus, M. T. Gamer, P. W. Roesky, *J. Organomet. Chem.* **2005**, *690*, 5078–5089; e) W. Maudez, M. Meuwly, K. M. Fromm, *Chem. Eur. J.* **2007**, *13*, 8302–8316; f) C. Ruspic, J. Spielmann, S. Harder, *Inorg. Chem.* **2007**, *46*, 5320–5326; g) S. Datta, M. T. Gamer, P. W. Roesky, *Organometallics* **2008**, *27*, 1207–1213; h) B. Liu, T. Roisnel, L. Maron, J.-F. Carpentier, Y. Sarazin, *Chem. Eur. J.* **2013**, *19*, 3986–3994; i) I. V. Basalov, B. Liu, T. Roisnel, A. V. Cherkasov, G. K. Fukin, J.-F. Carpentier, Y. Sarazin, A. A. Trifonov, *Organometallics* **2016**, *35*, 3261–3271; j) X. Sun, T. Simler, K. Reiter, F. Weigend, P. W. Roesky, *Chem. Eur. J.* **2020**, *26*, 14888–14895.
- [58] K. M. Fromm, *Coord. Chem. Rev.* **2020**, *408*, 213193.
- [59] S. Labouille, C. Clavaguéra, F. Nief, *Organometallics* **2013**, *32*, 1265–1271.
- [60] S. Grimme, J. Antony, S. Ehrlich, H. Krieg, *J. Chem. Phys.* **2010**, *132*, 154104.
- [61] a) J. P. Perdew, *Phys. Rev. B: Condens. Matter Mater. Phys.* **1986**, *33*, 8822–8824; b) A. D. Becke, *Phys. Rev. A* **1988**, *38*, 3098–3100.
- [62] *TURBOMOLE Version 7.4, a development of University of Karlsruhe and Forschungszentrum Karlsruhe GmbH, 1989–2007, TURBOMOLE GmbH since 2007.*
- [63] R. Heinzmann, R. Ahlrichs, *Theor. Chim. Acta* **1976**, *42*, 33–45.
- [64] H.-L. Su, L. M. Pérez, S.-J. Lee, J. H. Reibenspies, H. S. Bazzi, D. E. Bergbreiter, *Organometallics* **2012**, *31*, 4063–4071.

---

Manuscript received: June 1, 2021

Accepted manuscript online: June 24, 2021

Version of record online: July 29, 2021